http://dx.doi.org/10.6113/TKPE.2016.21.6.465

독립형 마이크로그리드에서 비선형 부하에 대한 고품질 전압제어

Hung D. Dam[1], 이홍희†

Effective Voltage Quality Control under Nonlinear Loads in Islanded Microgrid

Hung D. Dam[1] and Hong-Hee Lee†

Abstract

A nonlinear load causes harmonic distortion and hampers the performance of other loads or distributed generation (DG) sources connected to the point of common coupling (PCC). This study proposes a new control strategy to reduce harmonic components, such as fifth and seventh harmonics, at the PCC under nonlinear loads in islanded microgrids, which comprise more than two DG sources. The proposed control scheme enables the DG source to share the power commanded by the control center as well as to compensate for the voltage harmonics at the PCC. The reference current is estimated from the voltage harmonics and injecting power; thus, the control scheme is implemented without any additional hardware devices. The simulation and experimental results are presented to verify the effectiveness of the proposed control method.

Key words: Harmonic, Microgrid, Nonlinear loads, Voltage quality control

1. Introduction

The Distributed Generation (DG) relying on the renewable energy resources becomes attractive in order to reduce the carbon emission and minimize the non-renewable resource to meet the epower demand. Microgrid concept using the coordinated control among the parallel DG interface converters has been popularized[1]-[3]. The output voltages of the DGs in ac microgrid are generally regarded as ideal sinusoidal voltage sources. However, in practical applications, it is hard to maintain the sinusoidal voltage because there are a large number of nonlinear or unbalanced loads in the three-phase microgrid such as single-phase loads, rectifier loads, adjustable-speed ac motor drivers and so on; if the network voltage harmonics are not treated properly, the voltage at the point of common coupling (PCC) point is highly distorted.

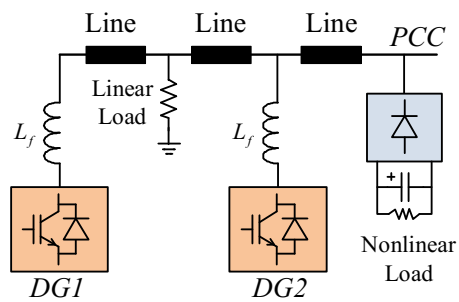

Fig. 1. Typical islanded ac microgrid configuration.

As well known, the power quality of the islanded microgrid can be deteriorated easily under the nonlinear loads since it lacks the voltage and frequency support from the grid[4]. Voltage distortion causes severe problems on the equipments such as vibration, over-voltage, and deteriorating the performance of the regulating converter. In order to

Paper number: TKPE-2016-21-6-2
Print ISSN: 1229-2214 Online ISSN: 2288-6281
† Corresponding author: hhlee@mail.ulsan.ac.kr, School of Electrical Eng., University of Ulsan.
Tel: +82-52-259-2187 Fax: +82-52-259-1686
[1] School of Electrical Eng., University of Ulsan
Manuscript received May 24, 2016; revised July 16, 2016; accepted Sep. 1, 2016

ensure the power quality in the utility, the active power filters (APFs) have been commonly utilized [5]-[8]. Especially, series APFs are usually utilized to compensate the voltage unbalance and harmonics by injecting harmonic voltage to the distribution line through the coupling transformers. However, the usage of APF increases the system cost as well as the complexity to achieve the coordinated operation of units in the system.

In order to compensate the PCC voltage of ac microgrid under the nonlinear loads, some control methods and topologies are introduced [4], [9]-[11]. In [4], authors proposed a grid-interfacing power quality compensator for the three-wire microgrid which contains two inverters (a shunt and a series). The shunt inverter is controlled to regulate the power dispatches among the parallel-connected DG systems, while the series inverter compensates the current by injecting appropriate voltage components. Authors in [9] implemented a grid-interfacing converter system by using the multiple proportional resonant controllers in order to enhance the voltage quality with the same configuration in [4]. Both [4] and [9] have complicate configurations, which leads the difficulty in the local control and the high cost in investment. To overcome these problems, Jinwei He et al. in [10] proposed a voltage-controlled method for the DG generation to compensate the voltage harmonics. With the conventional inverter configuration, the harmonic detector is added based on the sliding discrete Fourier transform, and the reference voltage is generated for the voltage loop control. This method solved the high cost problem, but it still requires a large amount of computation. Furthermore, the total harmonic distortion is not sufficiently reduced enough to meet IEEE 519 standard in [12].

To mitigate the cost and computation problems, this paper proposes a harmonic reduction method for the voltage source inverter under the microgrid application. Each DG is implemented by using the proposed control scheme to achieve two main functions: Sharing the loads with other DG to follow the command of the power management center, and reducing the harmonic components under the nonlinear load condition to improve the voltage quality at PCC. In order to verify the effectiveness of the proposed control scheme, simulation and experimental results are given.

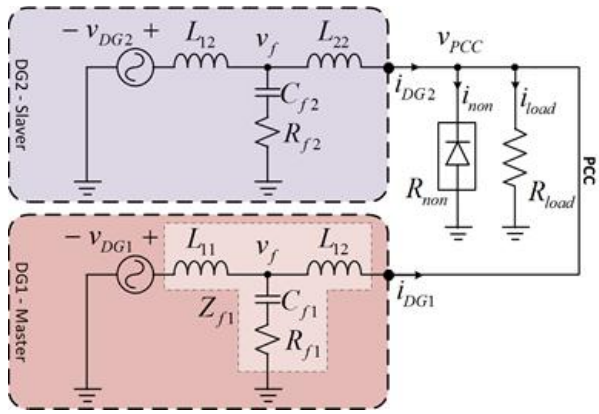

Fig. 2. Equivalent circuit of ac microgrid.

2. Proposed control strategy

2.1 Problems in microgrid under nonlinear loads

Fig. 2 shows a typical ac microgrid in islanded operation. All DG sources and nonlinear loads are connected to the PCC. In the master-slave operation, DG1 operates as a master with voltage source, and the remaining DGs operate as current source. Therefore, the equivalent circuit of an ac microgrid with two DG sources is shown in Fig. 2. Due to the nonlinear load R_{non}, the harmonic current i_{non} is drawn, and the distorted voltage V_{Zf1} is generated across the output impedance of DG1 without involving DG2. Then, the voltage at PCC becomes

$$V_{pcc} = V_{DG1} - Z_{f1} i_{DG1} \tag{1}$$

where i_{DG1} is the supplied current from DG1 and Z_{f1} is the equivalent filter impedance of DG1 . From the characteristic of three-phase nonlinear load, the harmonic current i_{non} generally consists of the $6n \pm 1 (n = 1, 2, ...)$ multiples of the fundamental frequency:

$$i_{non} = \sum_{h \neq 1} i_{non\_h} \tag{2}$$

where i_{non_h} is the h-th harmonic component of the nonlinear load.

Therefore, the voltage at PCC is distorted due to the harmonic components of the $6n \pm 1 (n = 1, 2, ...)$ multiples of the fundamental frequency [11]. In order to compensate the harmonic voltage at PCC, it is important to design an effective and low-cost current

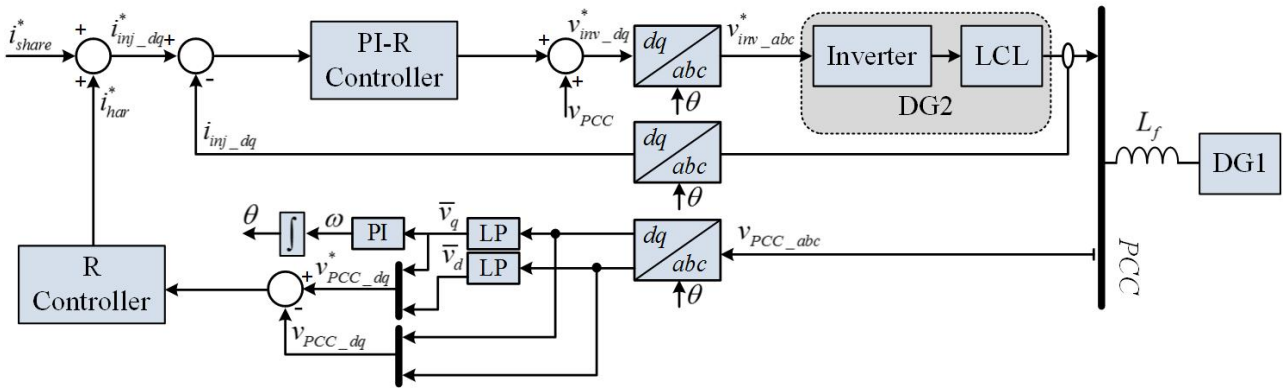

Fig. 3. Proposed control scheme for the VSI in DG.

controller that can generate the specific harmonic components to compensate the load current harmonics.

2.2 PCC Voltage harmonic reduction

The control scheme is responsible for producing an induced voltage to compensate the distorted voltage drop across the output impedance of other DG sources. In order to investigate the behavior of the harmonic components, the synchronous reference (d-q) frame rotating with the fundamental frequency ω_0 is used. In d-q frame, the $(6n\pm1)^{th}(n=1,2,...)$ harmonics are converted into the $(6n)^{th}(n=1,2,...)$ harmonics, so that the controller design becomes much easier. The block diagram of the proposed control scheme is shown in Fig. 3, which consists of one resonant controller (RC) and one proportional-integral-resonant controller (PI-R). The resonant controller is implemented in d-q frame rotating with the fundamental frequency ω_0 to generate the $(6n)^{th}(n=1,2,...)$ harmonic injecting current references i^*_{har}. The PI-R controller is also designed in d-q frame, and controls the output current of DG1 to follow the reference current which is the combination of sharing current i^*_{share} and harmonic currents i^*_{har}, where i^*_{share} is given by the control center so called power management center(PMS) based on the power provided by the main DG source and the power rating of each DG. The reference sharing current is determined to reduce the operating cost as well as to optimize the system operation[5].

3. Controller design

3.1. Modified Phase Locked Loop Design

Fig. 5 show the modified phase locked loop (PLL). In Fig. 5, two low-pass filters (LP) are added to filter out the d and q harmonic components of the PCC voltage, and they make the PLL operation stable under the distorted PCC voltage. After LP, the average voltages $\overline{v_d}$ and $\overline{v_q}$ become the reference values of the resonant controller to generate the reference harmonic currents as shown in Fig. 3.

The cut-off frequency of the LP in PLL is very important to satisfy the stability and dynamic performance of the whole system; low cut-off frequency leads to slow response, while high cut-off frequency makes the system unstable. In this paper, the cut-off frequency of LP is 10 rad/s, which is determined heuristically.

3.2. Determination of the controller gains

As shown in Fig. 3, there are two control loops, voltage and current loops. The voltage loop maintains the PCC voltage by generating the harmonic injecting components based on the sensed PCC voltage. The current loop controls the VSI to inject the current to the PCC corresponding to the reference current generated by the voltage loop and the power calculation. In order to ensure the robust operation of the controller, the following four components should be designed carefully: the band-width of resonant controller ω_c, the gain of resonant controller k_R, two gains of PI controller K_P and K_I.

3.2.1. Current control loop

The open loop transfer function of the PI-R controller used to control current is

$$G_c(s) = G_{PIR}(s)G_{LCL}(s)\ , \qquad (3)$$

where $G_{PIR}(s)$ and $G_{LCL}(s)$ are the transfer functions of PI-R controller and the LCL output filter

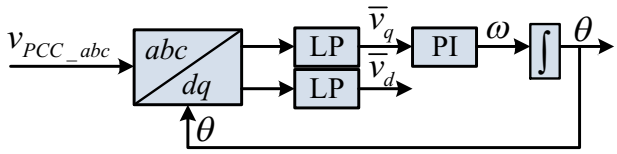

Fig. 4. Modified phase looked loop.

of DG, respectively, and they are given as following:

$$G_{PIR}(s)= K_P + \frac{K_I}{s} + \frac{k_r \omega_c s}{s^2 + 2\omega_c s + (h\omega_s)^2} \quad (4)$$

$$G_{LCL}(s)= \frac{C_f R_f s + 1}{C_f L_1 L_2 s^3 + C_f (L_1 + L_2) R_f s^2 + (L_1 + L_2) s} \quad (5)$$

where K_P is the proportional gain, K_I is the integral gain, k_r is the resonant gain, ω_c is the band-width of the resonant controller, ω_s is the fundamental frequency with $h = 6n, (n = 1,2,...)$, and C_f, L_1, L_2 and R_f are parameters of the LCL filter, respectively.

In (4), overall frequency characteristics of the PI-R controller depends on the gains K_P and K_I , while the gain k_r affects the PI-R response at the resonant frequencies. In order to find the PI gains, the effect of the current loop gains K_P and K_I is investigated when $k_r = 1$ by using the root loci. In Fig. 5(a), K_I should be smaller than 200 to ensure the system stable, while K_P can be any value. For further analysis, the Bode diagram of (4) is plotted with variation of K_P from 1 to 8 and K_I from 20 to 200 as shown in Fig. 5(b). In Fig. 5(b), as K_P increases, the cut-off frequency of control loop also increases. In order to reduce the effect of PI controller at the harmonic frequencies, the cut-off frequency should be lower than the 6-th harmonic frequency. Considering this point, we select $K_P = 2$, where the cut-off frequency is around 160Hz, which is low enough to remove the noises. Fig. 5(c) shows the relationship between K_I and the control loop phase delay, and the value $K_I = 100$ is selected to keep high gain and low phase delay at the fundamental frequency. Finally, the PI gaines for the current controller are given as $K_P = 2, K_I = 100$.

In order to adapt the fundamental frequency variation, the band-width of resonant controller, ω_c, is considered. Fig. 6 shows the Bode diagram of the

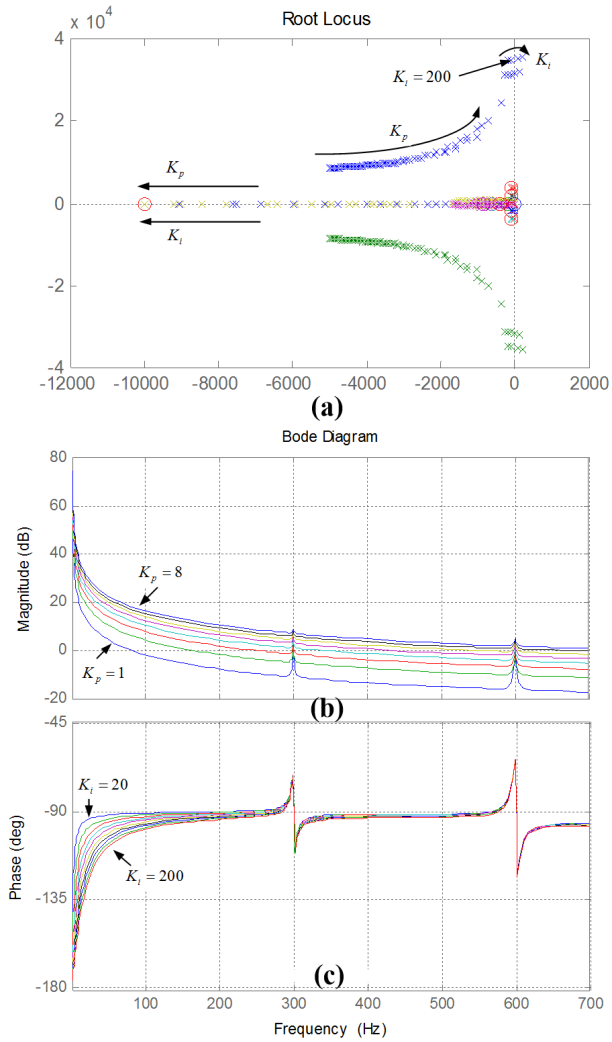

Fig. 5. The effect of current loop gains K_P and K_I.
(a) Root locus trajectory
(b) K_P effects on gain of control loop
(c) K_I effects on phase delay of control loop

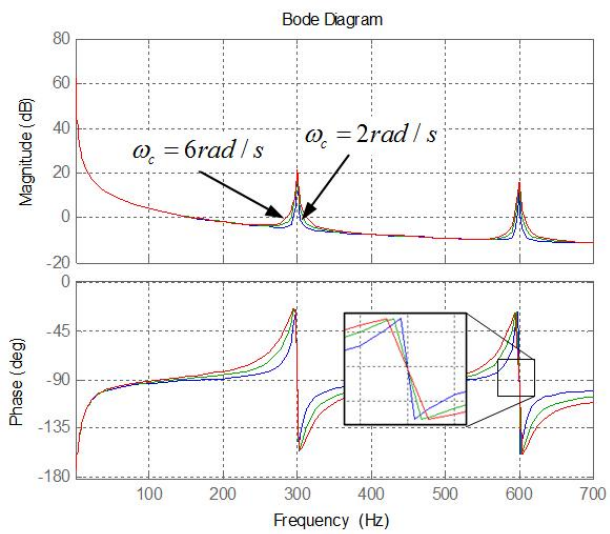

Fig. 6. Effect of band-width of resonant controller.

TABLE I
ISLANDED MICROGRID PARAMETERS

System parameters	Value
PCC Voltage	60Vrms, 50Hz
Linear Load	1.1kW
Nonlinear Load	300W
Inductance of DGs Filter	2mH

open-loop transfer function in (3) for the different band-width of the resonant controller, 2, 4, and 6 rad/s with the gains $K_P = 2, K_I = 100, k_r = 1$. In Fig. 6, the band-width of 6 rad/s provides less phase delay variation in spite of the fundamental frequency variation. In this study, the band-width is selected as $\omega_c = 6rad/s$ because it provides fast dynamic response of the controller and a good adaptive performance for the fundamental frequency variation.

The gain of the resonant controller affects the response time and the phase delay of the controller as well as the stability of the system. The higher gain makes the response time of the harmonic current controller faster. However, it easily leads the system to be unstable because the higher harmonic components can be injected to PCC bus. Therefore, to ensure the stable system, the gains of the resonant controller are not too high to prevent the output current from oscillating at the resonant frequency.

3.2.2. Voltage Control Loop

The voltage control loop generates the harmonic component reference i^*_{har} for the current control loop. The resonant controller (RC) for the voltage control loop has the following transfer function:

$$G_{H\_RC} = \frac{k_{Hr}\omega_c}{s^2 + 2\omega_c + (h\omega_s)^2} \quad , \qquad (6)$$

where k_{Hr} is the resonant gain, ω_c is the band-width of the resonant controller, ω_s is the fundamental frequency with $h = 6n, (n = 1, 2, ...)$. The gain of RC is chosen according to the magnitude of harmonic components. The higher gain of resonant controller generates higher harmonic current reference or injects higher harmonic currents to the PCC bus.

Fig. 7 shows Nyquist diagram of the control loop with the chosen PI gains. In Fig. 7, if the resonant gain of current loop is larger than 4 for the voltage control loop and 65 for the current control loop, the

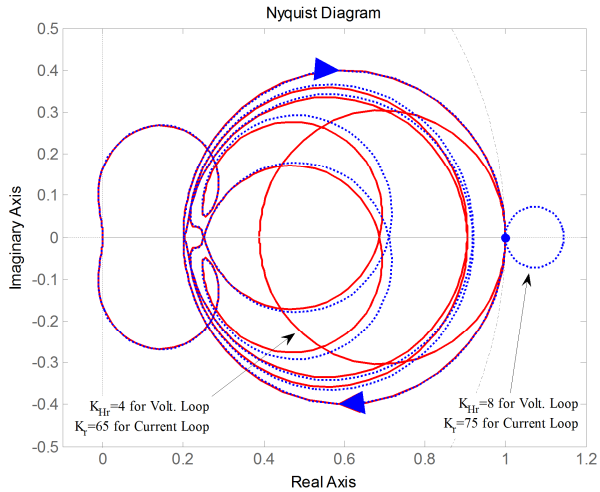

Fig. 7 . Nyquist diagram of control loop with difference of gains.

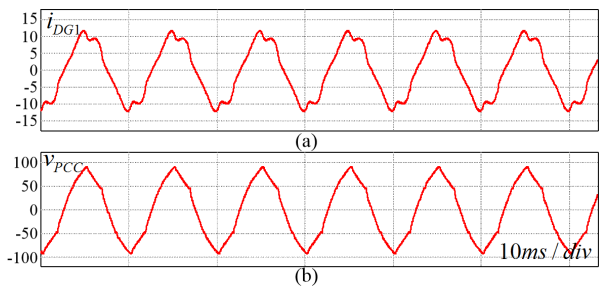

Fig. 8. Distorted phase voltage at PCC and output current without compensation method.

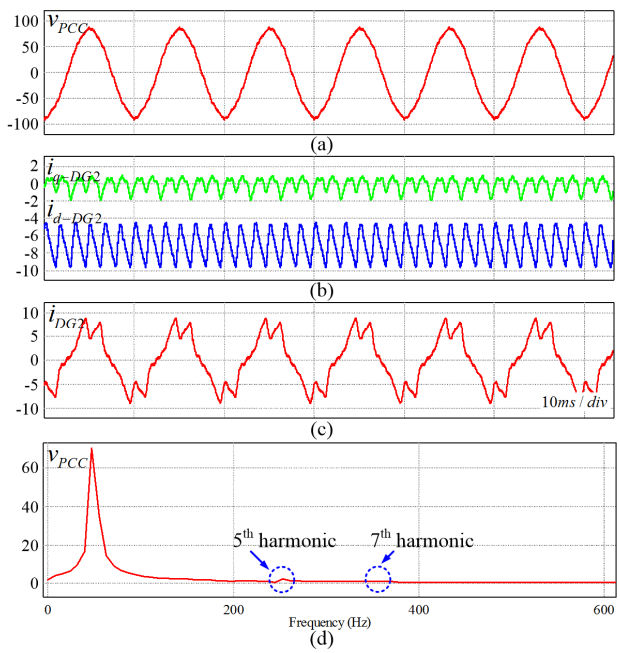

Fig. 9. Steady state performance proposed scheme.
(a) voltage waveform at PCC after compensation
(b) dq frame current of DG2
(c) output current of DG2
(d) PCC voltage harmonic spectrum

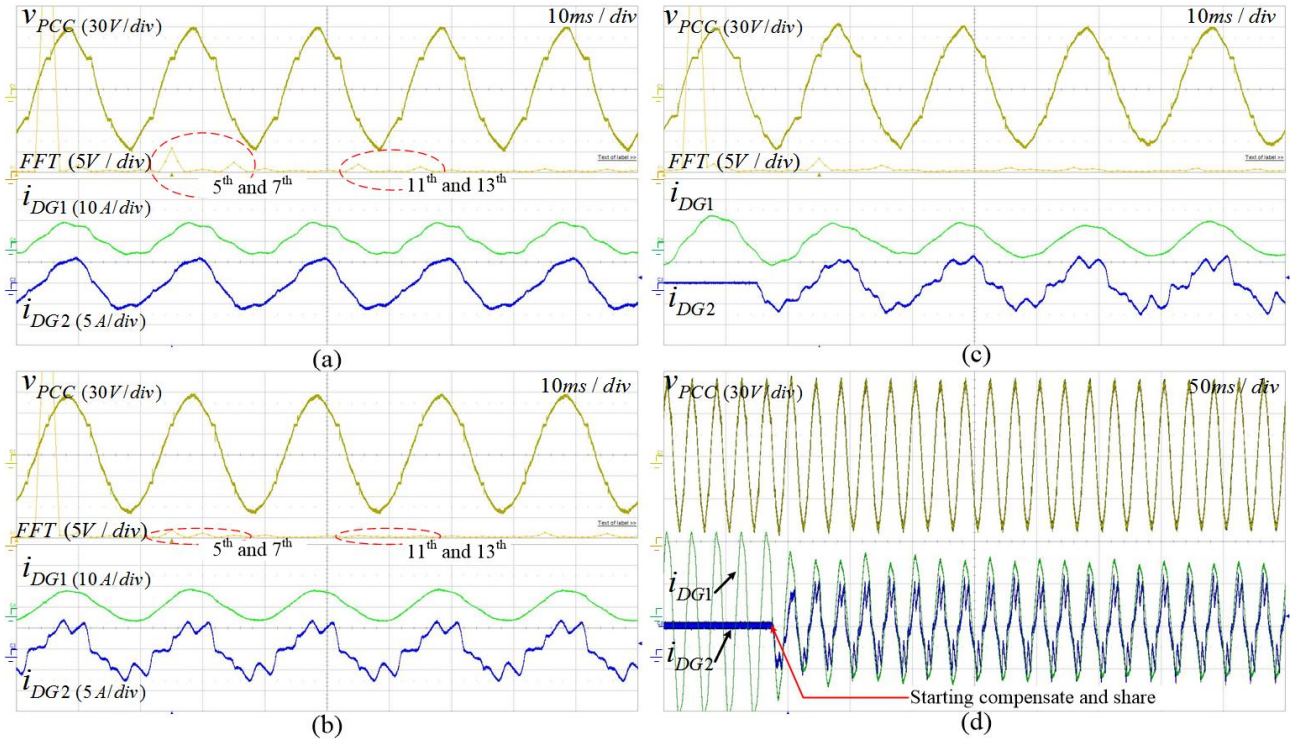

Fig. 10. PCC Voltage and DGs currents with
(a) conventional PI current control (b) proposed control scheme (c) proposed scheme - responses time
(d) proposed scheme - sharing loads power sharing

system can be unstable (the blue dotted line is out of unit circle). By considering the effect of the harmonic components, the resonant controller gains are determined as following when the non-linear load characteristics is given in Table 1: The current loop gains of the resonant controller are 65 for the 6-th harmonics and 25 for the 12-th harmonics, and the gains of voltage controller are 4 for 6-th harmonics and 3 for 12-th harmonics.

4. Simulation results

In order to verify the performance and effectiveness of the proposed control strategy, both simulation and experiments are carried out with a simple microgrid with 2 DG sources in Fig. 1. The simulation is performed using PSIM software. The voltage at PCC of ac microgrid is 60Vrms, 50Hz, and the load power demand is 1.4kW (including linear and nonlinear loads). The sharing current i^*_{share} is determined by the central controller according to the load condition and the DG's rating; in simulation, 7A peak value is applied. At the initial moment, the load is fed by DG1. After that, the DG2 shares the power with DG1, and also compensates the harmonic components at the PCC voltage.

Fig. 8 shows the PCC voltage and DG1 current when DG2 is controlled without any harmonic compensation; the PCC voltage and the DG1 current are distorted; the THD of PCC voltage is 9%.

The simulation results with the proposed control scheme are shown in Fig. 9, which shows that the PCC voltage is compensated with the reduced THD from 9% to 2.3%. Fig. 9(a) shows the sinusoidal waveform of the PCC voltage. In Fig. 9(b), the average currents of the d and q components are -7 and 0, respectively, which follow the reference values very well to share the load power properly. Fig. 9(d) shows the spectrum analysis of the PCC voltage, which shows that the 5-th and 7-th harmonic components are reduced to almost zero.

5. Experimental verifications

The experimental system is basically same as the configuration shown in Fig. 1. But, in experiment, the DG1 is replaced with AC programmable source Chroma 61704, and the DG2 is implemented by VSI which is controlled by the proposed scheme with the aid of DSP TMS320F28335. At the initial moment, the

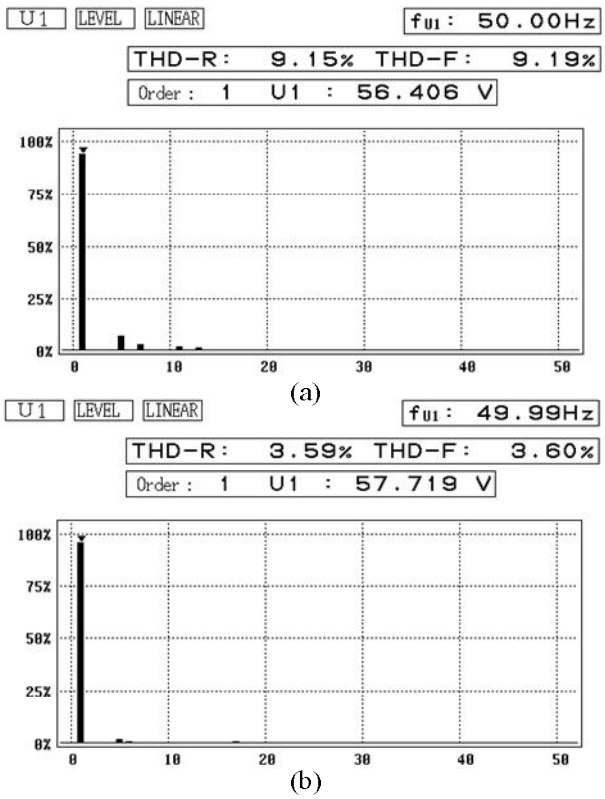

Fig. 11. THD of PCC voltage.
(a) without proposed control scheme (b) with proposed control scheme.

DG1 supplies the power to the local linear and nonlinear loads. After that, the DG2 starts to share the load power and to compensate the harmonic voltage at PCC with the sharing current of 5A peak value. The parameters of the microgrid are given in Table 1.

Fig. 10(a) shows the PCC voltage and DG's currents when DG2 is controlled with the conventional PI current controller. Without compensation, the PCC voltage is highly distorted; the output currents of both DGs are not sinusoidal.

The proposed control scheme is implemented by DG2 and the experimental results are shown in Figs. 10(b), (c), and (d). Fig. 10(b) shows the steady state performance of the proposed control scheme, where the PCC voltage waveform becomes almost sinusoidal, so that the 5-th and 7-th harmonic components are reduced to almost zero. Fig. 10(c) shows the response time of control scheme; it takes around 3 cycles to reach the steady state. In Fig. 10(d), the power sharing of the proposed control scheme are shown, and we can see that the injected current of DG2 is in phase with DG1 current and shares the power with DG1 properly.

The THD of the PCC voltage is 9.19% when DG2 is controlled by the conventional PI controller. However, the THD of the PCC voltage reduces to 3.60% with the proposed control scheme, which fully complies with the IEEE 519 standards in [12]. Fig. 11 shows the THD values measured by HIOKI 3193 Power Hitester, and the magnitude of the fundamental frequency is also increased with the proposed control scheme as shown in Fig. 11 because the dropped voltage on the output impedance of DG1 is compensated by DG2.

The experimental results show that proposed control scheme effectively compensates the PCC voltage as well as properly shares the power with other sources in the islanded microgrid. Even though the case study in this paper is carried out for the islanded microgrid with two DGs and only one DG is controlled with proposed control scheme, the proposed scheme can be applied to a larger scale of islanded ac microgrid with more than two DGs.

6. Conclusion

A harmonic compensation scheme at the PCC voltage in a stand-alone ac microgrid was proposed in this paper. With the proposed control scheme, the voltage harmonic components at PCC are effectively reduced without any additional hardware devices, and the load power is shared properly. The simulation and experimental results show the effectiveness of the proposed scheme, and it shows the possibility to apply to an islanded microgrid with multiple DGs.

This work was supported by the National Research Foundation of Korea Grant funded by the Korean Government (NRF-2015R1D1A1A09058166).

References

[1] R. H. Lasseter, "MicroGrids," in *Power Engineering Society Winter Meeting, 2002. IEEE,* Vol. 1, pp. 305-308, Aug. 2002.

[2] M. Barnes, J. Kondoh, H. Asano, J. Oyarzabal, G. Ventakaramanan, R. Lasseter, N. Hatziargyriou, and T. Green, "Real-world microgrids-an overview," in *System of Systems Engineering, 2007. SoSE '07. IEEE International Conference on*, pp. 1-8, Apr. 2007.

[3] F. Katiraei and M. R. Iravani, "Power management strategies for a microgrid with multiple distributed generation units," *Power Systems, IEEE Transactions on*, Vol. 21, No. 4, pp. 1821-1831, Nov. 2006.
[4] Y. W. Li, D. M. Vilathgamuwa, and P. C. Loh, "A grid-interfacing power quality compensator for three-phase three-wire microgrid applications," in *Power Electronics Specialists Conference, 2004. PESC '04. 2004 IEEE 35th Annual*, Vol. 3, pp. 2011-2017, Jun. 2004.
[5] H. Akagi, "New trends in active filters for power conditioning," *Industry Applications, IEEE Transactions on*, Vol. 32, No. 6, pp. 1312-1322, Nov. 1996.
[6] F. Z. Peng, "Application issues of active power filters," *Industry Applications Magazine, IEEE*, Vol. 4, No. 5, pp. 21-30, Sep. 1998.
[7] B. Singh, K. Al-Haddad, and A. Chandra, "A review of active filters for power quality improvement," *Industrial Electronics, IEEE Transactions on*, Vol. 46, No. 5, pp. 960-971, Oct. 1999.
[8] P. Mattavelli, "A closed-loop selective harmonic compensation for active filters," *Industry Applications, IEEE Transactions on*, Vol. 37, No. 1, pp. 81-89, 2001.
[9] F. Wang, J. L. Duarte, and M. A. M. Hendrix, "Grid-interfacing converter systems with enhanced voltage quality for microgrid application - concept and implementation," *Power Electronics, IEEE Transactions on*, Vol. 26, No. 12, pp. 3501-3513, Dec. 2011.
[10] J. W. He, Y. W. Li, and M. S. Munir, "A flexible harmonic control approach through voltage-controlled DG - Grid interfacing converters," *Industrial Electronics, IEEE Transactions on*, Vol. 59, No. 1, pp. 444-455, Jan. 2012.
[11] D. Menniti, A. Burgio, A. Pinnarelli, and N. Sorrentino, "Grid-interfacing active power filters to improve the power quality in a microgrid," in *Harmonics and Quality of Power, 2008. ICHQP 2008. 13th International Conference on*, pp. 1-6, Sep. 2008.
[12] "IEEE recommended practice and requirements for harmonic control in electric power systems," *IEEE Std 519-2014 (Revision of IEEE Std 519-1992)*, pp. 1-29 Jun. 2014.

Hung D. Dam

He was born in Thanh Hoa, Vietnam, in 1989. He received the B.S. degree Electrical Engineering from the Ho Chi Minh City University of Technology, Ho Chi Minh City, Vietnam, in 2012. Currently, he is an M.S./Ph.D. combined student at the University of Ulsan, Ulsan, Korea. His research interests are Renewable Energy Conversion Systems, Smart-grid.

Hong-Hee Lee

He received his B.S., M.S., and Ph.D. in Electrical Engineering from Seoul National University, Seoul, Korea, in 1980, 1982, and 1990, respectively. From 1994 to 1995, he was a Visiting Professor at the Texas A&M University. He has been a Professor in the School of Electrical Engineering in the Department of Electrical Engineering, University of Ulsan, Ulsan, Korea since 1985. He is also the Director of the Network-based Automation Research Center (NARC), which is sponsored by the Ministry of Trade, Industry and Energy. His research interests include power electronics, network-based motor control, and renewable energy. Dr. Lee is a member of the Institute of Electrical and Electronics Engineers (IEEE), the Korean Institute of Power Electronics (KIPE), the Korean Institute of Electrical Engineers (KIEE), and the Institute of Control, Robotics and Systems (ICROS). He was the President of KIPE in 2014.